J. Membrane Biol. 146, 101–111 (1995)

The Journal of
Membrane
Biology

Extracellular pH Modulates the Ca^{2+} Current Activated by Depletion of Intracellular Ca^{2+} Stores in Human Macrophages

A. Malayev, D.J. Nelson
The University of Chicago Departments of Neurology, Medicine, and Pharmacological and Physiological Sciences, Chicago, IL 60637

Received: 30 March 1994/Revised: 3 March 1995

Abstract. Intracellular Ca^{2+} (Ca_i) signaling following the binding of surface receptors activates a Ca^{2+} permeable plasma membrane conductance which has been shown to be associated with store depletion in a number of cell types. We examined the activation of this conductance in human monocyte-derived macrophages (HMDMs) using whole-cell voltage-clamp techniques coupled with fura-2 microfluorimetry and characterized the importance of external pH (pH_o) as a modulator of current amplitude. Current activation was observed following experimental maneuvers designed to deplete intracellular Ca^{2+}-stores including: (i) dialysis of the cell with 100 μM inositol 1,4,5-triphosphate (IP_3), (ii) intracellular dialysis with high concentrations of the Ca^{2+} buffers EGTA and BAPTA, or (iii) exposure of the cell to the Ca^{2+}-ATPase inhibitor thapsigargin (1 μM). Currents associated with store depletion were inwardly rectifying with kinetics, inactivation, and selectivity that appeared similar irrespective of the mode of activation. Currents were Ca^{2+} selective with a selectivity sequence of $Ca^{2+} > Sr^{2+} \gg Mg^{2+} = Mn^{2+} = Ni^{2+}$. The Ca^{2+} influx current was modulated by changes in pH_o; modulation was not produced as a consequence of changes in internal pH (pH_i). External acidification led to a reversible reduction in current amplitude with a pKa at pH 8.2. Changes in pH_o alone failed to induce current activation. These observations are consistent with a scheme by which changes in pH_o, as would be encountered by macrophages at sites of inflammation, could change the time course and magnitude of the Ca_i transient associated with receptor activation by regulating the influx of Ca^{2+} ions.

Key words: Macrophage activation — Inositol 1,4,5-trisphosphate — Calcium current — Protons — Thapsigargin — Inflammation

Correspondence to: D.J. Nelson

Introduction

Receptor activation of phospholipase C in macrophages results in a transient, biphasic rise in internal calcium (Ca_i) which appears to be due to both release from internal stores and influx across the plasma membrane. The initial phase of Ca^{2+} release is mediated via the activation of an inositol 1,4,5-trisphosphate (IP_3)-gated channel in the endoplasmic reticulum. The mechanism underlying the second phase, a sustained Ca^{2+} entry, is not yet clear. The observation that an inwardly rectifying, Ca^{2+}-selective current is activated in a number of cell types following experimental manipulations which lead to store depletion has led to the hypothesis that the signal which initiates the influx of Ca^{2+} is the state of refilling of the internal stores (Hoth & Penner, 1992; Bahnson, Pandol & Dionne, 1993; Hoth & Penner, 1993; McDonald, Premack & Gardner, 1993; Parekh, Terlau & Stuhmer 1993; Randeiamampita & Tsien, 1993; Zweifach & Lewis, 1993).

This study characterizes a similar inward conductance in human macrophages that is activated following any one of three experimental maneuvers designed to deplete intracellular calcium stores: (i) an increase in intracellular IP_3, (ii) dialysis of the cell with intracellular solutions of high Ca^{2+} buffering capacity, and (iii) exposure of the cell to the Ca^{2+}-ATPase inhibitor, thapsigargin. Hormone-activated Ca^{2+}-entry has been shown to be modulated by changes in pH_o (Blackmore et al., 1984; Muallem, Pandol & Beeker, 1989) reminiscent of proton modulation observed for a number of plasma membrane cation conductances (Hille, Woodhull & Shapiro, 1975; Iijima, Ciani & Hagiwara, 1986; Pietrobon, Prod'hom & Hess, 1988). Macrophages are inflamma-

tory cells commonly found at necrotic tissue sites where the pH_o may vary widely. In the microenvironment of abscesses, pH_o levels can fall to as low as 5.5 (Bryant et al. 1980). Therefore, our aim was an assessment of the importance of H^+ as a modulator of the Ca^{2+}-selective inward current activated upon store depletion in macrophages. Our observations suggest that small changes in extracellular pH as would be encountered by inflammatory cells contribute significantly to the modulation of the depletion-activated Ca^{2+} current and hence could play a role in regulating Ca^{2+} entry in cells at sites of inflammation.

Materials and Methods

Cell Culture

Mononuclear cells isolated from peripheral blood samples collected from healthy human volunteers were separated from neutrophils and erythrocytes by Ficoll-Hypaque density gradient centrifugation and maintained in long term culture as previously described (Nelson, Jow & Jow, 1990). Human monocyte-enriched leukocyte fractions, suspended in RPMI-1640 containing 10% autologous human serum 100 U/ml penicillin and 50 μg/ml streptomycin were cultured in teflon vials (Savillex, Minnetonka, MN) at 37°C in a 5% CO_2 air atmosphere prior to their introduction into adherent culture. Cells were maintained in suspension culture in teflon vials for 1–2 weeks and plated on glass-bottom culture dishes approximately 30 min prior to recording.

Dishes, which served as recording chambers, were constructed as previously described (Katnik & Nelson, 1993). In brief, an 18 mm diameter hole was punched into the bottom of a 35 mm plastic culture dish. A 22 × 22 mm, acid cleaned cover slip was fixed to the outside surface of dish covering the hole using Sylgard 184 silicone elastomer (Dow-Corning, Midland, MI). Dishes were placed in a drying oven at 55°C for 1 hr to allow for sufficient Sylgard curing. A drop of the mononuclear cell suspension (0.2 ml) was placed in the center of the exposed coverslip and incubated for 10 min at 37°C in a humidified 5% CO_2:95% O_2 environment. Following incubation and initial cell attachment, nonadherent cells were removed through washing with the external recording solution.

Solutions

The standard internal (pipette) solution contained (in mM): 100 Cs-glutamate, 50 CsCl, 1 EGTA-CsOH, 0.2 $CaCl_2$, 2 $MgCl_2$, 10 HEPES buffered to pH = 7.2. In some experiments, N-methyl-D-glucamine (NMDG) was used to replace some fraction of the Cs^+ with no observable effect on the activation properties of the inward conductance. In experiments requiring an internal solution with a high Ca^{2+} buffering capacity, 11 mM EGTA and 2 mM $CaCl_2$ were used in place of 1 EGTA and 0.2 $CaCl_2$. In the 11 mM EGTA containing solutions, the free Ca^{2+} was calculated to be 39 nM. In the 1 mM EGTA containing solutions, the free Ca^{2+} was calculated to be 43 nM. Free Ca^{2+} was calculated assuming an apparent dissociation constant for EGTA of 0.15 μM at pH 7.2 using the methodology of Fabiato and Fabiato (1979). The external (bathing) solution contained (in mM): 130 NaCl, 10 $CaCl_2$, 10 HEPES-NaOH, pH = 7.4. In experiments investigating the divalent selectivity of the inward conductance, $CaCl_2$ was exchanged for either 10 mM $MnCl_2$, $NiCl_2$, $MgCl_2$, or $SrCl_2$ in the external solution. In experiments in which the external pH was altered, the pH of the solutions was adjusted immediately before use. Solution osmolarities were monitored using a vapor pressure osmometer (Model 5500, Wescor, Logan, UT) and adjusted to 300 mOs.

BAPTA, tetrapotassium salt was obtained from Molecular Probes (Eugene, OR). Thapsigargin (Calbiochem, La Jolla, CA) and inositol 1,4,5-trisphosphate (IP_3) [LC Laboratories (Woburn, MA)] were stored at −20°C in stock solutions. Aliquots of the stock solutions were diluted in the appropriate experimental solutions immediately prior to use. Thapsigargin was stored in a DMSO stock solution while IP_3 was dissolved in the 11 EGTA containing pipette solution.

Electrophysiology

Whole-cell recordings from HMDMs were obtained using the techniques of Hamill et al. (1981). A dish containing cultured cells was placed in a chamber on the movable stage of an inverted microscope equipped with phase-contrast optics. Recordings pipettes were formed from borosilicate glass (World Precision Instruments, Sarasota, FL) using a horizontal puller (Model-P87, Sutter Instrument, San Rafael, CA). The resistance of the saline-filled pipettes was between 4-7 MΩ. Whole-cell currents were obtained using a List EPC-7 (List Electronic, Darmstadt, West Germany) voltage clamp. The output of the current-to-voltage converter was filtered through a low pass filter at 0.5 kHz. The current signal was sampled at 1 kHz and written into data files using an IBM-AT compatible.

In some experiments investigating the time course of current activation in the presence of internally dialyzed IP_3, voltage ramps from −100 to 100 mV (0.5 mV/msec) were applied from a holding potential of 0 mV at 5 sec intervals. The current record obtained in response to the first ramp was used as background current and was subtracted from the subsequent records. The current recorded at −45 mV was then used to monitor the time course of current activation. Step voltage protocols were also used in experiments in which the time course of current inactivation was studied. Voltage steps from a holding potential of 0 mV to command potentials between −100 to 50 mV were applied at 5-sec intervals. In general, currents recorded in the step voltage protocols were not leak or capacitance corrected unless stated otherwise. Peak currents in the current-voltage relationships were measured 20–40 msec after the initiation of the voltage pulse. Whole-cell current activation and inactivation was analyzed as a sum of exponentials by a Fourier method (Provencher, 1976) that determined the number, amplitudes, and time constants of the components.

In some experiments a bath perfusion system was employed which allowed for sequential solution changes. Bath solution changes were made at a rate of approximately 1 cc/min. In those experiments in which the external Cl^- was replaced by aspartate, the bath ground electrode was connected to the bath solution via an agar/saline bridge in order to prevent electrode offset potentials.

Microfluorimetry

Experiments were performed on a Leitz microscope equipped with UV transparent optics. Dye excitation illumination was provided by a Photon Technology International (PTI, South Brunswick, NJ 08852) D-101 dual wavelength illumination system. The D-101 consisted of a 75 watt xenon arc lamp, a variable speed reflective optical chopper and two monochromators both under computer control. The illumination system was coupled to the microscope via a fiber optic cable that mixed and randomized the output of the two monochromators over the field of view. Excitation light was deflected with a 450 nm dichroic mirror through a 40× phase (Nikon Fluor, N.A. 0.85) objective. Emitted fluorescence filtered at 510 nm was collected by a Hammamatsu R928

photomultiplier tube and photon-counting photometer through a variable rectangular aperture roughly equal to the area of the single cell. Photomultiplier output was sampled at 20 Hz and processed using a PTI interface on a NEC 386/20 personal computer. The monochromator slit widths were set at 12 nm.

Cells were loaded with fura-2 acetoxy methyl ester (5 μM) (Molecular Probes, Eugene, OR) for 1.5 hr at room temperature in RPMI buffered with 25 mM HEPES. This loading solution also contained 0.2% pluronic acid to obtain maximum dye dispersion and 0.5% bovine serum albumin (BSA) to prevent nonspecific dye binding. Following the loading procedure, cells were washed and incubated for 30 min with extracellular solution (in mM): 140 NaCl, 5.4 KCl, 2 $CaCl_2$, 2 $MgCl_2$, 10 HEPES, pH 7.4, to allow time for maximal dye deesterification. Cells were washed again prior to use. All experiments were performed within 2 hr after completion of fura-2 loading. Cells chosen for experiments were loaded to levels which were at least 10 times that measured for a cell-free area of the coverslip using the masking iris set to the size of the cell. Changes in Ca_i were expressed as the ratio (R) of dye fluorescence at 340 and 380 nm.

Experiments were carried out at room temperature. Summary data are expressed as means ± SEM with the number of experiments in parentheses.

Results

Activation of an Inward Current Following Depletion of Intracellular Ca^{2+} Stores

Whole-cell current recordings on human monocyte-derived macrophages (HMDMs) were made in extracellular solutions containing 10 Ca^{2+} and no K^+. Outward K^+ current was inhibited by the isosmolar substitution of Cs^+ or NMDG for K^+ in the intracellular solution. Under these ionic conditions, the inclusion of 100 μM inositol 1,4,5-trisphosphate (IP_3) in the pipette solution resulted in the activation of an inwardly rectifying current with a positive reversal potential which was similar in the depletion-activated Ca^{2+} entry current previously described in a number of cell types (Bahnson et al., 1993; Hoth & Penner, 1992; McDonald et al., 1993; Zweifach & Lewis, 1993). The time course of current activation was determined in experiments in which voltage ramps from −100 to 100 mV were delivered to the cell from a holding potential of 0 mV at 5 sec intervals. Examples of current records obtained in response to voltage ramps at 10 sec and 150 sec following the establishment of the whole-cell configuration are shown in Fig. 1*A*. Activation of the inward current was not dependent upon the presence of IP_3 in the pipette solution. Current activation was also observed in the presence of a variety of stimuli known to deplete internal Ca^{2+} stores including high internal concentrations of EGTA and BAPTA as well as the endoplasmic reticulum Ca^{2+}-ATPase inhibitor, thapsigargin. Data obtained in the presence of all the activation stimuli is summarized in the Table. Current activation occurred with a variable delay which was dependent upon the activation stimulus. In the case of IP_3,

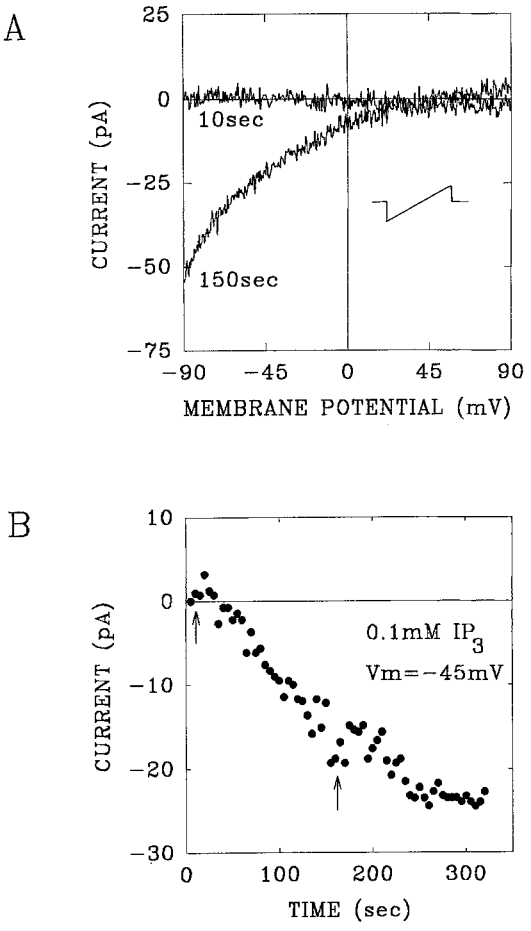

Fig. 1. Inward current activation by internal IP_3. (*A*) Whole-cell current recordings during voltage ramps from −100 to +100 mV from a holding potential of 0 mV obtained from the same cell. The pipette solution contained (mM): 100 NMDG-glutamate, 50 CsCl, 11 EGTA-CsOH, 2 $CaCl_2$, 2 $MgCl_2$, 10 HEPES, 0.1 IP_3, pH = 7.2. The external solution contained (mM): 10 $CaCl_2$, 130 NaCl, 10 HEPES, pH = 7.4. The first record, obtained just after establishing the whole-cell configuration, was used as leak current record and was subtracted from all subsequent records. Representative currents are shown at 10 and 150 sec after whole-cell formation. (*B*) The time course of inward current activation. Current magnitude determined at −45 mV elicited during voltage ramps from −100 to +100 mV delivered to the cell every 5 sec was used to construct the time course of current activation. The potential of −45 mV was chosen because it was close to the reversal potential of Cl^- and thus minimizes the possibility of a contribution from the activation of a Cl^- conductance. Arrows indicate points during the time course of activation at which current records in *A* were taken.

current was clearly detectable at 150 sec after establishing the whole-cell conformation reaching a steady-state level at approximately 300 sec (see Fig. 1*B*). The time constant for current activation was determined for all stimuli examined from fits to time course data as in Fig. 1*B* for IP_3. Current activation was well fit with a single exponential function. A comparison of the time constants for activation among the BAPTA-buffered solu-

Table 1. Comparative Ca^{2+} permeability and kinetic parameters of activation and inactivation for the depletion-activated Ca^{2+} conductance as a function of activation stimulus in HMDMs

Activation stimulus	[b]Current density (pA/pF)	[c]Increase in slope conductance with increasing $[Ca^{2+}]_0$	[d]$\tau_{activation}$ (in sec)
EGTA (11 mM)	2.54 ± 0.27 (n = 5)	1.35 ± 0.08 (n = 4)	ND
EGTA (1 mM) + [a]Th	ND	2.06 ± 0.33 (n = 5)	ND
EGTA (1 mM) + IP_3	2.57 ± 0.42 (n = 5)	1.94 ± 0.12 (n = 4)	85.0 ± 31.5 (n = 5)
BAPTA	1.31 ± 0.10 (n = 8)	1.36 ± 0.12 (n = 4)	261.0 ± 21.8 (n = 4)
BAPTA + Th	1.82 ± 0.41 (n = 4)	1.67 ± 0.19 (n = 4)	162.0 ± 54.0 (n = 5)
BAPTA + IP_3	2.45 ± 0.36 (n = 8)	2.07 ± 0.07 (n = 5)	119.0 ± 24.7 (n = 6)

Activation stimulus	[e]$\tau_{1\ inactivation}$ (in msec)	[e]$\tau_{2\ inactivation}$ (in msec)	[f]Percent current inactivation	Activation delay (in sec)
EGTA (11 mM)	13.1 ± 1.1 (n = 7)	164.7 ± 36.3 (n = 7)	67 ± 3.5 (n = 7)	177.0 ± 7.8 (n = 3)
EGTA (1 mM) + [a]Th	ND	230.8 ± 13.1 (n = 5)	ND	ND
EGTA (1 mM) + IP_3	8.5 ± 1.5 (n = 5)	139.0 ± 25.9 (n = 5)	63 ± 6.9 (n = 5)	70.0 ± 18.0 (n = 4)
BAPTA	13.3 ± 3.0 (n = 4)	116.5 ± 23.0 (n = 4)	63 ± 4.9 (n = 4)	278.0 ± 61.5 (n = 4)
BAPTA + Th	10.1 ± 3.3 (n = 3)	108.0 ± 3.0 (n = 3)	57 ± 8.2 (n = 3)	251.0 ± 45.1 (n = 5)
BAPTA + IP_3	11.9 ± 2.0 (n = 7)	110.2 ± 20.0 (n = 7)	60 ± 3.7 (n = 7)	45.0 ± 12.5 (n = 6)

Summary data are expressed as means ± SEM with the number of experiments in parenthesis. EGTA concentrations are as indicated; BAPTA was used at a concentration of 10 mM. In the studies conducted using EGTA and thapsigargin or IP_3 as a stimulus, the internal pipette solution contained 1 mM EGTA. The concentration of IP_3 was 100 μM.

[a] Thapsigargin (Th) was applied externally at a concentration of 1 μM.

[b] In the calculation of current density, capacitance was measured by integrating the current during a 10- to 20 mV voltage step and subtracting a baseline established about 20 msec after the step as determined from a nonlinear fit to the data. Current amplitude was determined as the peak current elicited at −100 mV following maximal current activation in the continued presence of the activation stimulus.

[c] Slope conductance was determined over the voltage range of −90 to −50 mV and is presented as the ratio of the conductance in 10 mM external Ca^{2+} to that in 2 mM external Ca^{2+}.

[d–e] The time course of current activation and inactivation was analyzed as a sum of exponentials by a Fourier method (Provencher, 1976) that determined the number, amplitudes, and time constants of the components. The time course of current activation (*see* text for description of measurement) was best fit by a single exponential function while current inactivation during a hyperpolarizing voltage pulse to −100 mV was best fit by a double exponential function.

[f] Percent current inactivation was determined as the ratio of the steady-state current at the end of a 500 msec, −100 mV voltage pulse to the amplitude of the peak current. The amplitude of the peak and steady-state currents were determined from exponential fits to the current data. All data were leak subtracted. ND indicates that determinations were not made.

tions demonstrated a significant decrease in $\tau_{activation}$ in the presence of IP_3 over that observed for BAPTA alone ($P \ll 0.05$).

Inward current activation was variably observed using pipette solutions which contained 11 mM EGTA as a depletion stimulus. The EGTA-induced current was observed in 40 of the 62 cells examined. The amplitude of the EGTA-induced current from a representative cell at 3 and 10 min is illustrated in Fig. 2*A* and *B*.

Time Dependence of Current Inactivation

The inwardly rectifying, depletion-activated current showed time-dependent inactivation during maintained hyperpolarizing voltage steps between −100 and −50 mV, as seen in Fig. 2*A* and *B*. Current inactivation was incomplete, leaving a significant steady-state current at the end of a 500 msec voltage pulse. The percentage decrease in current was similar for both Ca^{2+} buffers and

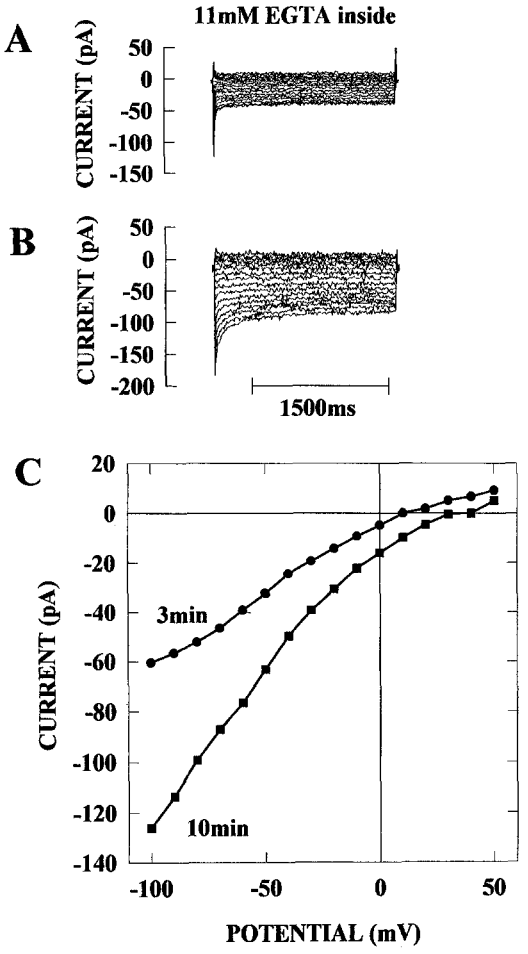

Fig. 2. Activation of inward current by EGTA. (*A*) Family of current records obtained in response to a series of voltage steps between −100 and +50 mV in 10 mV increments in the presence of 11 mM internal EGTA 3 min following whole-cell formation. The holding potential was 0 mV. (*B*) Current recording from the same cell 10 min following whole-cell formation. (*C*) The corresponding *I–V* relationship (filled circles for peak current at 3 min and filled squares for currents at 10 min) for the currents in *A* and *B*. The pipette solution contained (mM): 150 CsCl, 11 EGTA-CsOH, 2 $CaCl_2$, 2 $MgCl_2$, 10 HEPES, pH = 7.2. External solution contained (mM): 10 $CaCl_2$, 130 NaCl, 10 HEPES, pH = 7.4.

was independent of activation stimuli. This is in contrast to the observations of Hoth and Penner (1993) on the depletion-activated current in rat mast cells where the decrease in current amplitude in response to hyperpolarizing voltage pulses was dependent upon the Ca^{2+} buffer present.

The time course of current inactivation was best fit with a double exponential function. The slower of the two time constants describing current inactivation varied significantly as a function of the internal Ca^{2+} buffering capacity as well as the activation stimulus. A comparison of the kinetic parameters of activation and inactivation for the depletion-activated current as a function of activation stimulus is given in the Table.

Divalent Selectivity of the Depletion-Activated Inward Current

The Ca^{2+} permeability of the depletion-activated conductance was demonstrated in experiments in which increases in internal Ca^{2+} (Ca_i) were directly correlated with inward current following maximal conductance activation. The results of a representative experiment using the endoplasmic reticulum Ca^{2+}-ATPase inhibitor, thapsigargin (1 μM) as an activation stimulus are illustrated in Fig. 3. Cells were loaded with the membrane permeant form of the Ca^{2+}-sensitive dye, fura-2. Individual voltage-clamped cells were monitored photometrically following bath exposure to thapsigargin. At the peak of the thapsigargin-induced Ca_i transient, voltage pulses between −100 and +50 mV were delivered to the cell and the temporal correlation between transient increases in Ca^{2+} and inward current activation were monitored as seen in the insert to Fig. 3*A*.

The Ca^{2+} selectivity of the thapsigargin-activated inward conductance was determined following exchange of the external solution containing 10 mM Ca^{2+} for one containing 1 mM Ca^{2+}. Examples of current records and corresponding current-voltage (*I–V*) relationships obtained upon changing external Ca^{2+} are shown in Fig. 3*B-F*. The change in external Ca^{2+} from 10 to 1 mM resulted in a reversible decrease in the slope conductance measured during step voltage changes from −100 to 50 mV. The average increase in conductance over the voltage range of −90 to −50 mV following an increase in external Ca^{2+} for all the activation stimuli is summarized in the Table. A comparison of currents obtained with BAPTA containing internal solutions showed a significant increase in the slope conductance ratio in the presence of BAPTA plus IP_3 over that obtained using BAPTA alone ($P \ll 0.05$). A significant increase in current density was also observed in the presence of BAPTA plus IP_3 over that observed in the presence of BAPTA alone ($P \ll 0.05$).

To determine the relative divalent selectivity of the conductance, ion substitution experiments were performed in which the external solution containing 10 mM Ca^{2+} was exchanged for a solution containing an equivalent concentration of either Sr^{2+}, Mg^{2+}, Mn^{2+}, or Ni^{2+}. In these experiments, thapsigargin (1 μM) was used to induce inward current activation. A comparison of the *I–V* relationship in a single cell in the presence of each of the divalent cations can be seen in Fig. 4. The relative divalent selectivity of the depletion-activated Ca^{2+} current was $Ca^{2+} > Sr^{2+} \gg Mg^{2+} = Mn^{2+} = Ni^{2+}$ as determined in 2 cells in which all divalents were tested.

The relative permeability of the depletion-activated conductance to the monovalent cation Na^+ was examined in experiments in which the external solution was exchanged for one in which Na^+ had been isosmotically replaced with the impermeant cation NMDG. Results of

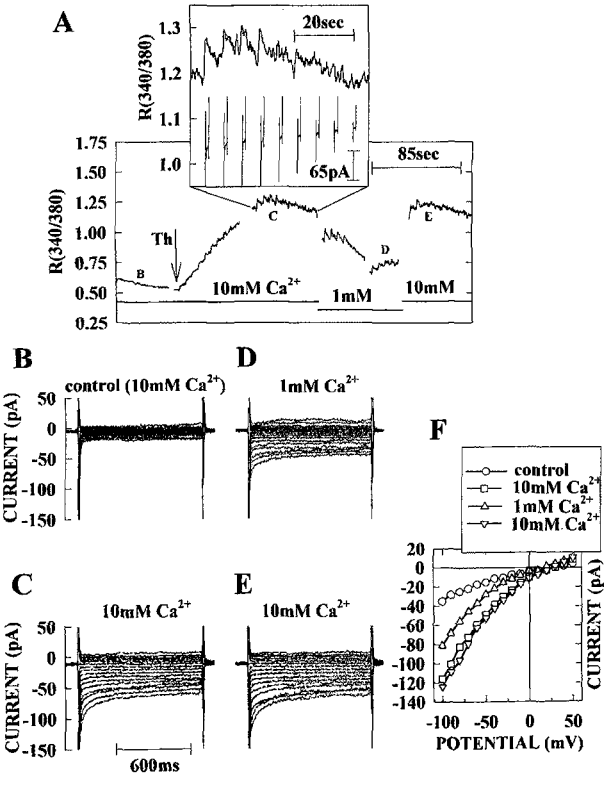

Fig. 3. Calcium permeability of the depletion-activated conductance in response to externally applied thapsigargin (Th). (*A*) Whole-cell currents and changes in Ca_i recorded in a cell dialyzed with a pipette solution containing pentapotassium fura-2 (100 μM). The internal pipette solution contained (mM): 100 Cs-glutamate, 50 CsCl, 1 EGTA, 0.2 $CaCl_2$, 2 $MgCl_2$, 10 HEPES. Thapsigargin (1 μM) was added to the bath solution at the arrow; an increase in Ca_i was monitored as the increase in the ratio of the fluorescence measured at 340 nm to that measured at 380 nm. A family of voltage pulses between −100 and +50 mV from a holding potential of 0 mV were applied to the preparation at the peak of the Ca_i response. Changes in external Ca^{2+} concentration are indicated by the labelled bars below the fluorescence trace. *Insert:* The inward current elicited during the voltage pulses seen plotted below the fluorescence trace was temporally correlated with transient increases in Ca_i. The more hyperpolarizing pulses were correlated with larger increases in inward current and larger increases in Ca_i. (*B*) Family of whole-cell currents in response to voltage pulses between −100 and +50 prior to exposure of the cell to thapsigargin (current records were recorded at the time point indicated as *B* in the fluorescence trace in *A*). The holding potential was 0 mV; the interpulse interval was 5 sec. The external solution contained 10 mM Ca^{2+}. The voltage protocol is identical for current records in *B* through *E*. (*C*) Current records taken during the peak of the thapsigargin induced increase in Ca_i; individual current traces are also given in the insert in *A*. (*D*) Current records following exchange of the external solution for one containing 1 mM Ca^{2+}. (*E*) Current traces following exchange of the bath solution to one containing 10 mM Ca^{2+}. (*F*) Corresponding *I–V* curves for the currents in *B* through *E*.

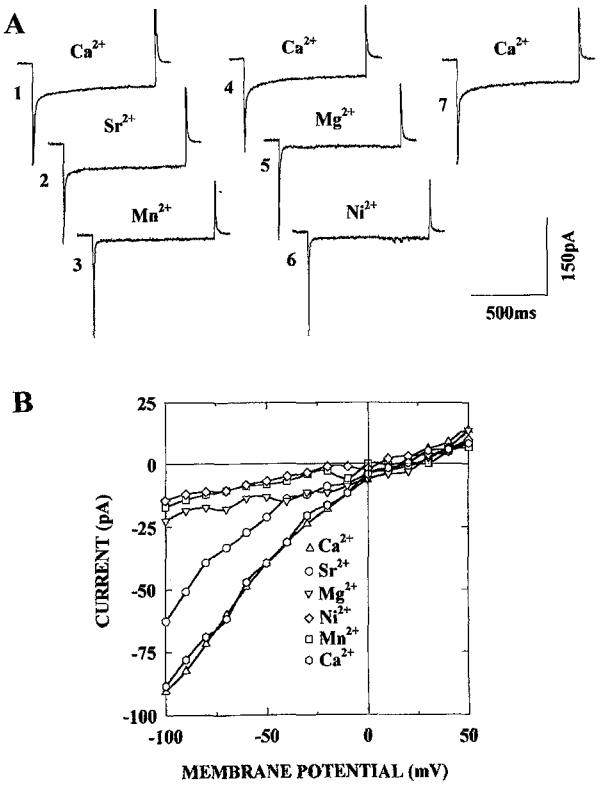

Fig. 4. Divalent permeability of the inward Ca^{2+} current activated by thapsigargin (1 μM). (*A*) Current traces obtained in response to membrane hyperpolarization to −100 mV from a holding potential of 0 mV. Extracellular Ca^{2+} (10 mM) was replaced with a series of divalents as indicated above each record. The number to the left of each trace corresponds to the order in which the traces were obtained. Current inhibition in the presence of blocking divalents was readily reversible upon returning to Ca^{2+}-containing external solutions as indicated in traces 1, 4, and 7. (*B*) *I–V* relationships obtained in the same cell. Voltage protocol was the same as that described in Fig. 2. Peak inward current was determined after exchange of the external solution containing 10 mM Ca^{2+} for one in which Ca^{2+} was replaced with an equimolar concentration of Ni^{2+}, Mn^{2+}, Mg^{2+}, and Sr^{2+}. Open diamonds indicate the *I–V* relationship in the presence of Ca^{2+} at the beginning of the experiment; open hexagons represent the *I–V* relationship in external Ca^{2+} at the end of the divalent substitution series and demonstrate the reversibility of the response.

a representative experiment are given in Fig. 5. As can be determined in the *I–V* relationships presented in Fig. 5*D*, current amplitude was unaffected by removal of external Na^+ indicating that (i) Na^+ is not significantly permeable through channels activated upon store depletion and (ii) there is no significant contribution of Na^+/Ca^{2+} exchange current to the conductance activated following store depletion.

Modulation of Inward Current Following Changes in External pH

Changes in the pH of the external solution over the pH range of 5.0 to 9.0 altered the magnitude of the inward conductance in a reversible manner. The amplitude of the inward current carried by Ca^{2+} at a given membrane potential increased as the external pH was increased, and

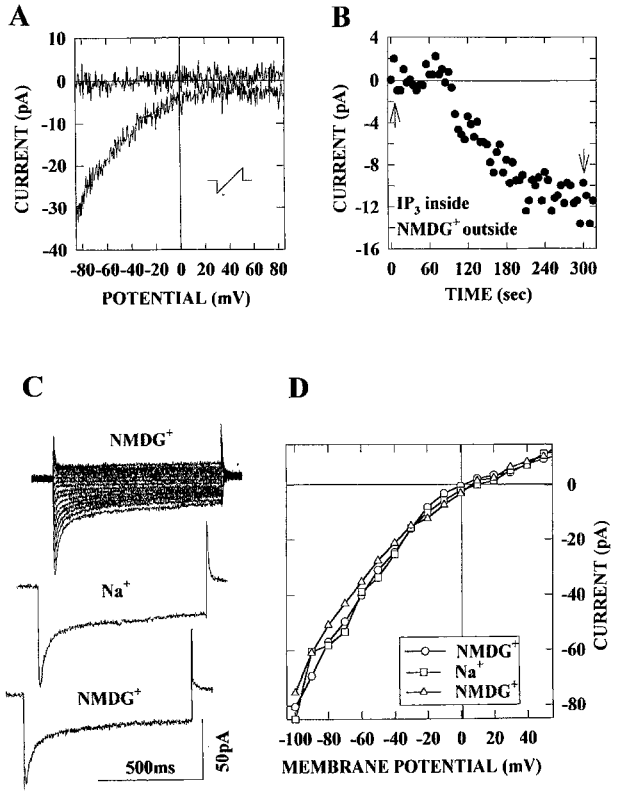

Fig. 5. Dependence of IP_3-induced current amplitude on external Na^+. (*A*) Whole-cell current recordings during voltage ramps from −100 to +100 mV from a holding potential of 0 mV in the absence of extracellular Na^+. The pipette solution contained (mM): 100 Cs-glutamate, 50 CsCl, 11 EGTA-CsOH, 1 $CaCl_2$, 1 $MgCl_2$, 10 HEPES, 0.1 IP_3, pH = 7.2. The external solution contained (mM): 10 $CaCl_2$, 130 NMDG-Cl, 10 HEPES, pH = 7.4. The first record, obtained just after establishing the whole-cell configuration, was used as leak current record and was subtracted from all subsequent records. Representative currents are shown at 10 and 300 sec after whole-cell formation. (*B*) The time course of inward current activation. Current magnitude at −45 mV elicited during voltage ramps delivered to the cell every 5 sec was used to construct the time course of current activation. Arrows indicate points during the time course of activation at which current records in *A* were taken. (*C*) Current record from the same cell after the current had reached steady-state level elicited using a step voltage protocol similar to that described in Fig. 2. The family of current traces was obtained in the presence of the Na^+ substitute NMDG. Individual current traces at 100 mV following substitution of the extracellular solution for one containing 130 mM NaCl and the subsequent exchange of the solution of one containing 130 mM NMDG-Cl are given below the initial family of current traces in 130 NMDG-Cl. (*D*) I–V relationship for the peak currents from records in *C*. Note the superposition of the *I–V* relationships; open circles indicate the *I–V* relationship initially obtained in the NMDG-containing external solution.

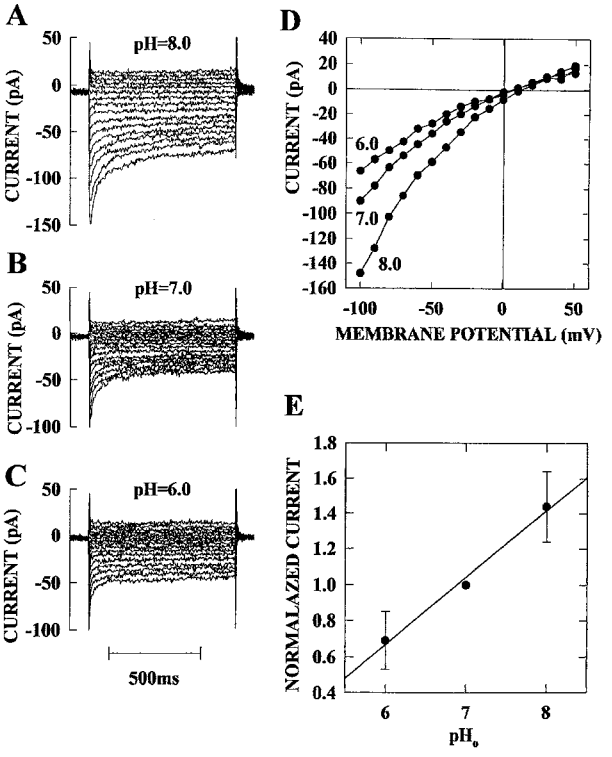

Fig. 6. Effect of external protons on the amplitude of the IP_3-induced inward Ca^{2+} current. (*A–C*) Current records obtained from the same cell at three different values of pH_o indicated above each set of current records. (*D*) Corresponding *I–V* curves for the peak currents in *A* through *C*. Internal and external solutions are identical to those in Fig. 1. (*E*) Summary of the proton-induced changes in the IP_3-induced inward Ca^{2+} current. Fractional changes in peak current amplitude at pH 8.0 and pH 6.0 was determined at −90 mV relative to current amplitude obtained at pH 7.0. Data were pooled from a total of 7 cells for pH changes from 7.0 to 8.0 and 4 cells for pH changes from 7.0 to 6.0. Error bars indicate SD.

decreased as the external pH was reduced. Proton modulation of the inward Ca^{2+} current in the presence of IP_3 (100 μM) is illustrated in Fig. 6. The current records at pH 6.0, 7.0, and 8.0 were obtained in a single cell. The amplitude of the inward current at −90 mV and pH 7.0 was 0.69 ± 0.2 (n = 7) times lower relative to that measured at pH = 8.0 and 1.44 ± 0.16 (n = 4) times higher as compared to that measured at pH_o = 6.0. A summary of the pH_o-induced modulation of the IP_3-induced inward Ca^{2+} current in the presence of 1 mM EGTA is given in Fig. 6*E*.

Figure 7 shows the effect of changes in external pH on the amplitude of the inward current activated by thapsigargin (1 μM) using internal solutions containing 10 mM BAPTA. In these experiments, BAPTA was used to prevent Ca^{2+}-dependent current inactivation and to ensure that changes in external pH were not modulating current amplitude via concomitant changes in Ca_i. When the pH_o was raised beyond 9 the depletion-activated current lost its characteristic rectification properties, thus, making it difficult to differentiate the depletion current from leak current and making it impossible to determine a plateau in the dose-response relationship. Data were pooled from 11 different cells. The smooth line through the data points represents the best fit of the data to a single site binding curve and yields of pKa of 8.2.

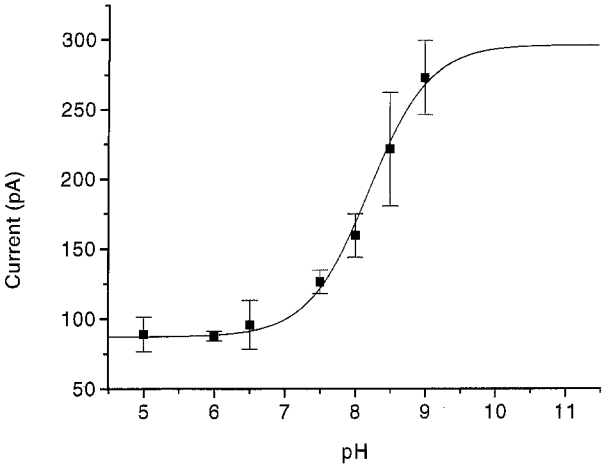

Fig. 7. Dependence of thapsigargin-induced inward current amplitude on external pH. Currents were measured using internal pipette solutions buffered with 10 mM BAPTA to reduce Ca^{2+}-dependent current inactivation. The internal pipette solution contained (mM): 100 CsCl, 40 Cs-glutamate, 10 BAPTA, 2 $MgCl_2$, 10 HEPES, 0.001 thapsigargin, pH 7.2. The external solution contained (mM): 130 NaCl, 10 $CaCl_2$, 2 $MgCl_2$, 10 HEPES buffered to the desired pH. The y-axis represents peak current amplitude at −100 mV. Currents were not leak corrected. The response to changes in extracellular pH was examined after currents had reached steady-state amplitude. Cell capacitance ranged from 50 to 86 pF in the 11 cells examined. Data points are expressed as mean ± SEM. Each data point represents a mean of between 3 and 11 cells. The smooth line through the data points represents the best fit of the data to a single-site binding curve with a pKa of 8.2 ± 0.1. The maximum current increase obtained from the fit to the data was 210 ± 26 pA.

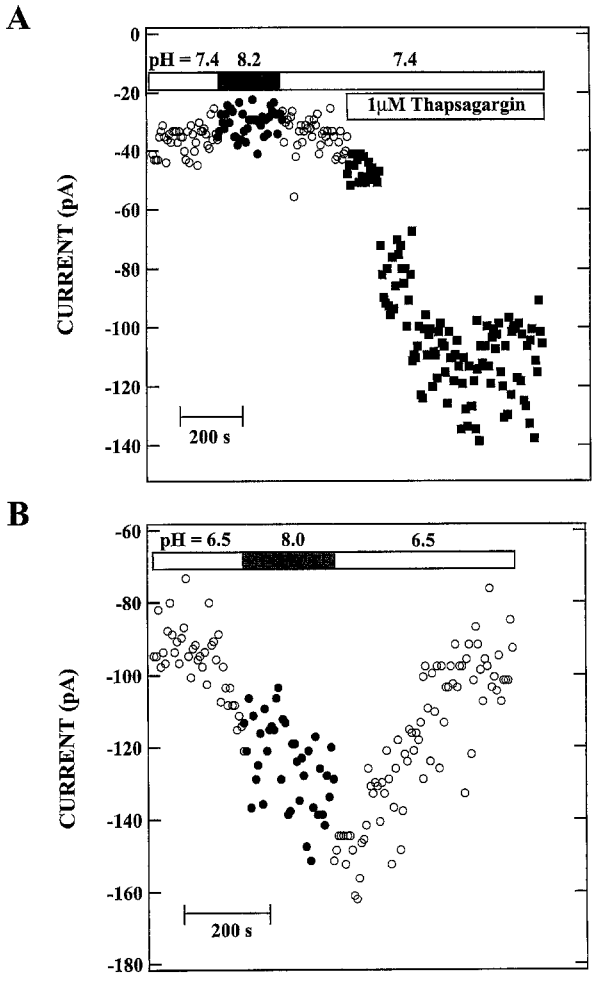

Fig. 8. Evidence that changes in pH_o alone do not induce current activation and that proton modulation of thapsigargin-induced inward current was reversible. (*A*) Peak current amplitude was determined during voltage steps to −100 mV from a holding potential of 0 mV at 5 sec intervals. Prior to thapsigargin-induced current activation, the external solution was exchanged from the standard external solution to solutions in which the pH was varied from pH 7.4 to pH 8.2 as indicated by the bars above the appropriate portion of the current record. Thapsigargin (1 μM) was added to the bath solution at pH 7.4 in order to induce maximal current activation. The average increase in current amplitude following exposure to thapsigargin was 73.6 ± 6.3 pA (n = 3). The pipette solution contained (in mM): 100 NMDG-glutamate, 40 CsCl, 1 EGTA, 0.2 $CaCl_2$, 2 $MgCl_2$, 10 HEPES. The bath solution contained (in mM): 130 Na-aspartate, 10 $CaCl_2$, 2 $MgCl_2$, and 10 HEPES. (*B*) Depletion-induced current following maximal activation in the presence of 1 μM thapsigargin. The pipette solution contained (in mM): 100 NMDG-glutamate, 40 CsCl, 10 Cs-BAPTA, 2 $MgCl_2$ 10 HEPES. The bath solution contained (in mM): 130 Na-aspartate, 10 $CaCl_2$, 2 $MgCl_2$, and 10 HEPES. Peak current amplitude as a function of time was determined during voltage steps to −100 mV as in (*A*). Exchanging the external solution from pH 6.5 to 8.0 was accompanied by an increase in current amplitude which was reversible upon returning the solution to pH 6.5.

Increases in extracellular pH alone failed to activate the depletion-activated current. When the pH of the external solution was increased prior to current activation, there was no observable change in current amplitude as can be seen in Fig. 8*A*. Similar results were obtained in 8 cells.

The proton-induced modulation of the thapsigargin-induced inward current was reversible upon return of the solution to pH 6.5 following exposure to an alkaline pH of 8.0, as seen in Fig. 8*B*. Data in Fig. 8*B* are representative of data obtained in 8 cells using both high EGTA and thapsigargin as activation stimuli.

We considered the possibility that the observed change in current magnitude with changes in pH_o could have occurred as an indirect result of changes in intracellular pH (pH_i). To buffer possible changes in internal pH in the face of changes in pH_o, experiments were carried out in the presence of 100 mM HEPES and 11 mM EGTA plus 100 μM IP_3 in the pipette solution. The time course of the development of the IP_3-induced inward Ca^{2+} current at −100 mV in an external solution of pH 8.2 is shown in Fig. 9*B*. The presence of increased pH buffering capacity in the internal/pipette solution did not abrogate inward current activation in alkaline solutions nor did it alter the current response to a decrease in pH_o to 7.4. The data in Fig. 9 are representative of observations made in 11 cells using both EGTA and IP_3 plus EGTA (11 mM) as activation stimuli. The average in-

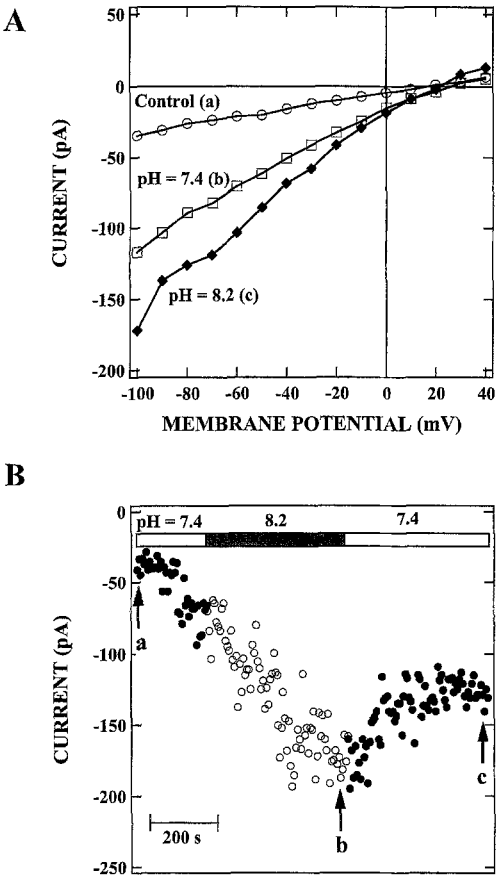

Fig. 9. Inward current activation is not due to changes in internal pH. (*A*) *I–V* relationships during step voltage protocols as in Fig. 2 from a cell dialyzed with 11 mM EGTA and 100 μM IP_3. The pipette solution contained (in mM): 40 CsCl, 60 NMDG-glutamate, 11 EGTA, 0.2 $CaCl_2$, 2 $MgCl_2$, 100 HEPES and 100 μM IP_3. The external solution contained (in mM): 130 Na-asparate, 10 $CaCl_2$, 10 HEPES. (*B*) Time course of current activation in the presence of high intracellular EGTA and IP_3 at elevated extracellular pH. Arrows indicate points at which the *I–V* curves in *A* were obtained.

crease in EGTA-activated current at –45 mV was 1.5 ± 0.2 fold (n = 4) in the presence of the high pH buffering capacity internal solutions and 1.65 ± 0.2 fold (n = 4) for currents obtained under the same conditions in the presence of low pH buffering capacity internal solutions.

Discussion

This study describes an inward Ca^{2+} conductance which is activated in HMDMs following experimental maneuvers designed to deplete intracellular Ca^{2+} stores. Inward current was activated in the presence of intracellular IP_3, although a qualitatively similar conductance could be activated in the absence of internal IP_3 but in the presence of high level of Ca^{2+} buffer or after external application of thapsigargin, an inhibitor of the endoplasmic Ca^{2+}-ATPase. Taken together these observations support the conclusion that Ca^{2+}-selective conductance which we observed in our studies is activated through the depletion of internal, IP_3-sensitive Ca^{2+} stores.

The "depletion activated" current or I_{CRAC} (Hoth & Penner, 1992) is similar in both conductance and kinetic properties to the current which we describe in the macrophage and provides a mechanistic basis for the depletion hypothesis or "capacitive" model for Ca^{2+} influx in nonexcitable cells first proposed by Putney (1990). The precise cytoplasmic signal which couples endoplasmic reticulum Ca^{2+} content to the plasma membrane is unknown. Recent data from secretory cells suggest that intracellular levels of cGMP may serve as a regulatory signal (Bahnson et al., 1993). An alternative candidate coupling molecule has been described in the recent studies of Randriamampita and Tsien (1993) which characterized a small (M_r = 500) soluble mediator termed CIF (Ca^{2+}-influx factor) which is released from intracellular organelles of stimulated lymphocytes. CIF appears to be released into the cytoplasm and to a much lesser extent the extracellular medium and increases Ca^{2+}-influx when applied to a number of cell types.

Parekh and colleagues have recently demonstrated in *Xenopus* oocytes that activation of expressed 5-HT receptors activates a divalent entry pathway similar to the store depletion-activated current characterized in a variety of nonexcitable cells. The 5-HT receptor-induced activation of the store depletion current appears to involve both a phosphatase and an unidentified diffusible messenger (Parekh et al., 1993).

The depletion-activated current which we characterized in HMDMs differs in its apparent Ca^{2+}-dependent inactivation as described for I_{CRAC} in mast cells (Hoth & Penner, 1993). We were unable to observe a significant effect of the internal buffering capacity on the extent of current inactivation in macrophages as has been reported for the mast cell. In macrophages after full depletion-current activation, the instantaneous current that developed in response to hyperpolarizations to –100 mV decreased by approximately 63% in the presence of BAPTA. In contrast, the decrease in inward current in mast cells in the presence of BAPTA was only 30% (Hoth & Penner, 1993). The decay of the depletion-activated current was fit as a double exponential. The fastest time constant did not vary significantly across all activation stimuli examined. The longest of the two time constants was dependent upon the activation stimulus and complimentary Ca^{2+} buffer, e.g., 108 ± 3 msec in the presence of BAPTA plus thapsigargin as compared to 231 ± 13 msec observed in the presence of 1 mM EGTA plus thapsigargin ($P \ll 0.001$).

We examined the comparative effect of IP_3 and thapsigargin on the time course of current activation in macrophages in the BAPTA containing solutions. The

time constant for current activation was not significantly increased in the presence of IP_3 over that observed for thapsigargin ($P > 0.05$); however, the presence of either IP_3 or thapsigargin significantly increased the time course of current activation over that observed for BAPTA alone ($P \ll 0.05$). In contrast, the time course for activation in mast cells was relatively constant for all activation stimuli (Hoth & Penner 1993). These differences suggest that perhaps the population or populations of channels activated upon store-depletion in HMDMs may differ in conductance and/or activation kinetics from those observed in mast cells. It may also suggest that there may be a rate-limiting activation step in the signal transduction process in HMDMs that is not present in the smaller mast cells. The mean mast cell capacitance in the studies of Hoth and Penner (1993) was 7.8 pF while the average capacitance of the HMDMs in our studies was 60.7 ± 2.4 pF (n = 67). In spite of the differences in kinetics, the divalent selectivity sequence for the depletion-activated current for both cell types was identical indicating that it represents a major pathway for Ca^{2+} influx following receptor activation in macrophages as well as mast cells.

Proton Modulation of Depletion Current in Macrophages

Changes in pH_o significantly and reversibly altered the amplitude of the inward Ca^{2+} conductance observed in the macrophage experiments. Increasing pH_o from 7.0 to 9.0 increased current magnitude across the voltage-range; conversely, decreasing pH_o from 7.0 to 5.0 decreased current magnitude. The modulatory effects of changes in pH_o were voltage-independent and were similar regardless of the pathway used to induce current activation. The mechanism by which extracellular protons decrease inward current carried by external Ca^{2+} remains unresolved in these studies. One possible mechanism to explain the proton-induced reduction in inward current amplitude would be that protons might be acting as fast channel blockers as has been observed for single cardiac Na^+ channels (Zhang & Siegelbaum, 1991). Such a mechanism would predict reversibility of the modulation with a relatively rapid time course. Alternatively, the reduction in current amplitude could also be due to a reduction in the negative surface potential as has been observed for the voltage-activated Ca^{2+} channel (Iijima et al., 1986). Single channel analysis would allow one to differentiate experimentally between proton effects on channel gating, conductance, or block. However, the depletion-activated Ca^{2+} influx channel has an estimated single channel conductance of approximately 24 fS (Zweifach & Lewis, 1993) making it difficult to examine directly at the single channel level. The fact that the changes in depletion-current in response to alterations of pH_o were not abrogated in experiments in which the pH buffering capacity of the cytoplasmic solution was increased, strongly suggests that the modulatory effects are due to direct interactions with the channel protein itself and not indirect via changes in internal pH. Our experiments, however, do not allow us to determine the precise nature of the interaction.

The inhibitory effects of external acidification were dependent on the concentration of protons with a pKa at pH 8.2. The pKa of the α-NH_3 group of cysteine is 8.3. The similarity in the pKas may suggest that a thiol-containing domain may be involved in determining proton binding and thereby current modulation.

The modulation of the Ca^{2+} influx channel by protons may be an intrinsic protective mechanism by which Ca^{2+} influx into inflammatory cells is regulated in the acidic extracellular environment characteristic of abscesses and tumors. A similar phenomenon may also help prevent neurons from irreversible hypoxic/ischemic injury via an inhibition of Ca^{2+} influx through the *N*-methyl-D-asparate (NMDA) channel (Tang, Dichter & Morad, 1990). The concentration dependence of the proton-induced inhibition of the depletion-activated current in the macrophage makes the channels highly sensitive to relatively small perturbations in external H^+ in the pH range normally encountered by the phagocyte. Thus, the acidic extracellular milieu at sites of inflammation may provide an important local feedback mechanism serving to limit Ca^{2+} entry into the activated phagocyte.

The authors wish to gratefully acknowledge the expert technical assistance of Weiwen Xie without whom the study could not have been completed. This work was supported by National Institutes of Health GM36823.

References

Bahnson, T.D., Pandol, S.J., Dionne, V.E. 1993. Cyclic GMP modulates depletion-activated Ca^{2+} entry in pancreatic acinar cells. *J. Biol. Chem.* **268:**10808–10812

Blackmore, P.F., Waynick, L.E., Blackman, G.E., Graham, C.W., Sherry, R.S. 1984. α- and β-adrenergic stimulation of parenchymal cell Ca^{2+} influx. *J. Biol. Chem.* **259:**12322–12325

Bryant, R.E., Rashad, A.L., Mazza, J.A., Hammond, D. 1980. β-lactamase activity in human pus. *J. Infect. Dis.* **142:**594–601

Fabiato, A., Fabiato, F. 1979. Calculator programs for computing the composition of the solutions containing multiple metals and ligands used for experiments in skinned muscle cells. *J. Physiol.* **79:**463–505

Hamill, O.P., Marty, A., Neher, E., Sakmann, B. 1981. Improved patch-clamp techniques for high resolution current recording from cells and cell-free membrane patches. *Pfluegers Arch.* **391:**85–100

Hille, B., Woodhull, A.M., Shapiro, B.I. 1975. Negative surface charge near sodium channels of nerve: divalent ions, monovalent ions, and pH. *Phil. Tran. R. Soc. London* **270:**301–318

Hoth, M., Penner, R. 1992. Depletion of intracellular calcium stores activates a calcium current in mast cells. *Nature* **355:**353–356

Hoth, M., Penner, R. 1993. Calcium release-activated calcium current in rat mast cells. *J. Physiol.* **465:**359–386

Iijima, T., Ciani, S., Hagiwara, S. 1986. Effects of the external pH on Ca channels: experimental studies and theoretical considerations using a two-site, two-ion model. *Proc. Nat. Acad. Sci. USA* **83:**654–658

Katnik, D., Nelson, D.J. 1993. Platelet activating factor-induced increase in cytosolic calcium and transmembrane current in human macrophages. *J. Membrane Biol.* **134:**213–224

McDonald, T.V., Premack, B.A., Gardner, P. 1993. Flash photolysis of caged inositol 1,4,5-trisphosphate activates plasma membrane calcium current in human T cells. *J. Biol. Chem.* **268:**3889–3896

Muallem, S., Pandol, S.J., Beeker, T.G. 1989. Modulation of agonist-activated calcium influx by extracellular pH in rat pancreatic acini. *Am. Phys. Soc.* **257:**G917–G924

Nelson, D.J., Jow, B., Jow, F. 1990. Whole-cell currents in macrophages. I. Human monocyte-derived macrophages. *J. Membrane Biol.* **117:**29–44

Parekh, A.B., Terlau, H., Stuhmer, W. 1993. Depletion of $InsP_3$ stores activates a Ca^{2+} and K^+ current by means of a phosphatase and a diffusible messenger. *Nature* **364:**814–818

Pietrobon, D., Prod'hom, B., Hess, P. 1988. Conformational changes associated with ion permeation in L-type calcium channels. *Nature* **333:**373–376

Provencher, S.W. 1976. A Fourier method for the analysis of exponential decay curves. *Biophys. J.* **16:**27–41

Putney, J.W.J. 1990. Capacitative calcium entry revisited. *Cell Calcium* **11:**611–624

Randriamampita, C., Tsien, R. 1993. Emptying of intracellular Ca^{2+} stores releases a novel small messenger that stimulates Ca^{2+} influx. *Nature* **364:**809–814

Tang, C.-M., Dichter, M., Morad, M. 1990. Modulation of the N-methyl-D-aspartate channel by extracellular H^+. *Proc. Natl. Acad. Sci. USA* **87:**6445–6449

Zhang, J.-F., Siegelbaum, S.A. 1991. Effects of external protons on single cardiac sodium channels from guinea pig ventricular myocytes. *J. Gen. Physiol.* **98:**1065–1083

Zweifach, A., Lewis, R.S. 1993. Mitogen-regulated Ca^{2+} current of T lymphocytes is activated by depletion of intracellular Ca^{2+} cells. *Proc. Natl. Acad. Sci. USA* **90:**6295–6299